Investigation of the Glyoxysome–Peroxisome Transition in Germinating Cucumber Cotyledons Using Double-label Immunoelectron Microscopy

DAVID E. TITUS and WAYNE M. BECKER
Department of Botany, University of Wisconsin, Madison, Wisconsin 53706. Dr. Titus' present address is Department of Tropical Public Health, Harvard School of Public Health, Boston, Massachusetts 02115.

ABSTRACT Microbodies in the cotyledons of cucumber seedlings perform two successive metabolic functions during early postgerminative development. During the first 4 or 5 d, glyoxylate cycle enzymes accumulate in microbodies called glyoxysomes. Beginning at about day 3, light-induced activities of enzymes involved in photorespiratory glycolate metabolism accumulate rapidly in microbodies. As the cotyledonary microbodies undergo a functional transition from glyoxysomal to peroxisomal metabolism, both sets of enzymes are present at the same time, either within two distinct populations of microbodies with different functions or within a single population of microbodies with a dual function.

We have used protein A-gold immunoelectron microscopy to detect two glyoxylate cycle enzymes, isocitrate lyase (ICL) and malate synthase, and two glycolate pathway enzymes, serine:glyoxylate aminotransferase (SGAT) and hydroxypyruvate reductase, in microbodies of transition-stage (day 4) cotyledons. Double-label immunoelectron microscopy was used to demonstrate directly the co-existence of ICL and SGAT within individual microbodies, thereby discrediting the two-population hypothesis. Quantitation of protein A-gold labeling density confirmed that labeling was specific for microbodies. Quantitation of immunolabeling for ICL or SGAT in microbodies adjacent to lipid bodies, to chloroplasts, or to both organelles revealed very similar labeling densities in these three categories, suggesting that concentrations of glyoxysomal and peroxisomal enzymes in transition-stage microbodies probably cannot be predicted based on the apparent associations of microbodies with other organelles.

During the first week after germination of cucurbits and other seeds containing fatty cotyledons, microbodies in the cotyledonary cells perform two distinct functions in succession. From shortly after germination through about day 5 of growth, the microbodies of cucumber cotyledons contain enzymes that function in β-oxidation of fatty acids and in the glyoxylate cycle. These organelles are accordingly called glyoxysomes (4). Activities of glyoxysomal enzymes such as isocitrate lyase (ICL)[1] and malate synthase (MS) rise to a peak at about day 4 and decline thereafter (1). Beginning at about day three, enzymes associated with the photorespiratory glycolate pathway accumulate in microbodies in a light-dependent manner as the cotyledons develop into green photosynthetic tissue. Microbodies containing characteristic photorespiratory enzymes such as hydroxypyruvate reductase (HPR), serine:glyoxylate aminotransferase (SGAT), and glycolate oxidase (GO) are called peroxisomes (25).

Although peroxisomes and glyoxysomes differ in function, they are indistinguishable ultrastructurally and have not been successfully resolved by subcellular fractionation from transitional tissue containing both types of activities (5, 11). Electron micrographs frequently reveal microbodies in close association with lipid bodies during the period of rapid lipid degradation (days 1–4 under our growth conditions). With the onset of photorespiratory metabolism (day 4 and later),

[1] *Abbreviations used in this paper:* GO, glycolate oxidase; HPR, hydroxypyruvate reductase; ICL, isocitrate lyase; MS, malate synthase; SGAT, serine:glyoxylate aminotransferase; TBST buffer, 10 mM Tris-HCl, pH 7.2, 500 mM NaCl, 0.3% (vol/vol) Tween-20; TBST+BSA buffer, TBST buffer containing 1% (wt/vol) BSA; TKME buffer, 150 mM Tricine, pH 7.5, 10 mM KCl, 1 mM $MgCl_2$, 1 mM EDTA.

THE JOURNAL OF CELL BIOLOGY · VOLUME 101 OCTOBER 1985 1288–1299

microbodies are often found appressed to chloroplasts (26). These spatial associations have been considered indicative of the functions performed by microbodies and therefore diagnostic of the enzyme complement of specific microbodies (i.e., a microbody adjacent to a lipid body would be presumed to contain glyoxysomal enzyme activities) (21, 22, 26).

The nature of the transition from glyoxysomal to peroxisomal function in cotyledonary microbodies remains poorly understood despite contributions from a number of laboratories over the past twelve years. Three models for this transition have been proposed. The two-population model (2) suggests that these distinct metabolic functions are sequestered into two populations of microbodies that differ biochemically but are otherwise indistinguishable. Two alternative models propose that the enzymes catalyzing these functions co-exist in a single population of microbodies. The first of these latter two models postulates that the changeover in microbody enzyme composition is accomplished by the gradual replacement of glyoxysomal enzymes by peroxisomal enzymes in a continually intact organelle (26). The third model suggests that microbodies are continually degraded and resynthesized, and that the enzymic contents of microbodies reflect the changing pattern of enzyme synthesis in the cell as development progresses (21).

Various biochemical and ultrastructural approaches have been applied to this controversy but have not succeeded in distinguishing between these three models for the glyoxysome-peroxisome transition. An attractive experimental strategy is to determine if glyoxysomal and peroxisomal enzymes can be found within the same microbody. Burke and Trelease (6) used enzyme cytochemistry at the electron microscope level to demonstrate that MS and GO are each present in >90% of microbody profiles at the time of transition from glyoxysomal to peroxisomal function in cucumber cotyledons. Although their results strongly suggested that these glyoxysomal and peroxisomal marker enzymes co-exist in the same microbodies, the cytochemical technique they used did not allow a direct, definitive demonstration of co-existence (2).

We have used immunocytochemistry to localize glyoxysomal and peroxisomal marker enzymes (ICL or MS, and SGAT or HPR, respectively) in transition-stage (day 4) cucumber cotyledons. The co-existence of ICL and SGAT in individual microbodies was directly demonstrated by double-label immunocytochemistry using two sizes of protein A-gold (10, 20).

MATERIALS AND METHODS

Sources: Protein A was obtained from Pharmacia Fine Chemicals, Piscataway, NJ. Lowicryl K4M resin was purchased from Polysciences, Inc., Warrington, PA. Miracloth was obtained from Calbiochem-Behring Corp., La Jolla, CA. Bovine serum albumin (BSA), polyethylene glycol, and $HAuCl_4$ were products of Sigma Chemical Co., St. Louis, MO.

Growth Conditions and Enzyme Assays: Cucumber seedlings (*Cucumis sativus* var. Improved Long Green) were grown at 25 ± 1°C for 1–8 d either in the dark or in continuous light. Samples of 20–30 cotyledons harvested from dry seeds and from each day of growth were frozen in liquid N_2 and stored at −70°C. Samples were thawed in buffer containing 150 mM Tricine, pH 7.5, 10 mM KCl, 1 mM $MgCl_2$, 1 mM EDTA (TKME buffer), homogenized with a Polytron homogenizer, centrifuged for 10 min at 20,000 *g*, and filtered through Miracloth. The resultant supernatants were assayed for ICL (17), MS (19), HPR (24), and SGAT (24) according to published procedures.

Antibody Preparation: The microbody enzymes ICL (17), MS (19), HPR (24), and SGAT (12) were purified from cucumber cotyledonary extracts as previously described. Monospecific antisera were raised in rabbits against a native preparation of HPR and SDS-denatured preparations of ICL, MS, and SGAT. Antisera to ICL (17), MS (19), and HPR (24) detect single bands on SDS gels of cotyledonary extracts. Anti-SGAT serum recognizes two bands on SDS polyacrylamide gels, one at 45 kD and the other at 47 kD. The two bands co-purify and behave as characteristic markers of peroxisomal development, though we have thus far been unable to determine whether one or both of the bands exhibit SGAT activity (12).

For immunocytochemical labeling, antisera were diluted in 10 mM Tris-HCl, pH 7.2, 500 mM NaCl, 0.3% (vol/vol) Tween-20 (TBST buffer) which also contained 1% (wt/vol) bovine serum albumin (BSA). Final dilutions were 1:100 for anti-MS and anti-HPR, 1:200 for anti-SGAT, and 1:2,000 for anti-ICL.

Protein A–Gold Preparation: Colloidal gold particles of two discrete size classes were prepared from $HAuCl_4$ according to published procedures. The citrate method of Frens was used for 20-nm particles (8) while 10–15-nm particles were prepared according to Horisberger (13). Colloidal gold preparations were stabilized with protein A, pelleted, resuspended in 10 mM Tris-HCl, pH 7.2, 150 mM NaCl, and 0.05% (wt/vol) polyethylene glycol, mixed with an equal volume of glycerol, and stored at −20°C. The 10-nm particles were obtained by fractionation of 10–15-nm particles on a 10–30% (wt/wt) sucrose gradient. For immunocytochemical labelings, protein A-gold was diluted with TBST buffer until a pale red color was achieved.

Electron Microscopy and Immunocytochemistry: Light-grown cucumber cotyledons were harvested at days 2, 4, and 8 post-germination and sliced perpendicular to the long axis into 0.5–1.0-mm sections in a drop of 50 mM potassium phosphate buffer (pH 7.0) containing 0.5% (vol/vol) glutaraldehyde and 4% (wt/vol) freshly prepared formaldehyde. Slices were then vacuum infiltrated, fixed for 2 h at 4°C in 1 ml of fixative solution, quickly rinsed twice with 2-ml aliquots of phosphate buffer, and dehydrated in an acetone series as follows: 10 min in 30% (vol/vol) acetone at 0°C followed by 30 min each in 50, 70, and 95% (vol/vol) acetone at −16°C. Tissue slices were infiltrated with successive 12-h steps at −16°C in 1:3, 2:2, and 3:1 (vol/vol) mixtures of Lowicryl K4M resin and 95% acetone. Dehydration and infiltration steps were performed on a rotating mixer to help overcome the inherent infiltration problems with cotyledonary tissue. The ratios of Lowicryl K4M components were 3.1 g crosslinker A + 16.9 g monomer B + 0.1 g initiator C. After 6 or more days in 100% resin, tissue slices were transferred to gelatin capsules and polymerized under UV light for 1 d at −16°C followed by 2 d at 25°C. Thin sections, silver-gold in color, were cut on a Sorvall MT-2 microtome and picked up on carbon- and Formvar-coated nickel grids.

Double-label immunocytochemistry was performed using a modification of the technique of Geuze et al. (10). Grids were floated for 10 min on 30-μl drops of TBST buffer containing 1% (wt/vol) BSA (TBST + BSA buffer), transferred into 30-μl drops of the first antiserum for 1 h, and then washed. Washing consisted of a 10-min incubation in a drop of TBST + BSA buffer (following antiserum steps) or TBST buffer (after protein A and protein A-gold steps) followed by a 40-s immersion in 20 ml of a stirred TBST buffer solution. Grids were then placed in drops of 10 nm protein A-gold for 30 min, transferred into a solution of protein A (0.2 mg/ml in TBST buffer) for 10 min, washed in TBST buffer, and then incubated in drops of the second antiserum for 1 h. Grids were washed in TBST + BSA buffer followed by TBST buffer, incubated in 20 nm protein A-gold for 30 min, washed in TBST buffer, and finally washed in triple-distilled H_2O before drying. For single-labeling experiments, the initial incubation in TBST + BSA buffer was followed directly by the steps used for the second antiserum (above). Poststaining was accomplished with 5 min in saturated aqueous uranyl acetate and 1–3 min in Reynolds' lead citrate.

Control experiments included substitution of preimmune sera for immune sera and immunostainings of tissue known to lack the specific antigens.

Quantitation of Immunocytochemical Labeling: Thin sections from tissue blocks containing spongy mesophyll cells were picked up on 200 square mesh grids and immunolabeled with either anti-ICL or anti-SGAT serum followed by 20 nm protein A-gold. For each grid, one mesh entirely covered by a section was selected at random and photographed as a series of 12 micrographs at a magnification of 3,000. The organellar specificity of gold labeling was estimated by counting gold particles in the first two micrographs of each series and assigning each gold particle to the appropriate underlying cell structure. Intercellular spaces were disregarded since gold particles were rarely if ever found in these areas. The areas of cell structures were determined with a digitizing tablet linked to an Apple computer, and densities of gold deposition were expressed as particles/μm^2.

To determine if the density of ICL or SGAT labeling over individual microbodies correlated with their proximity to other specific organelles, microbody profiles were scored for number of gold particles, cross-sectional area, and the presence or absence of adjacent lipid bodies, chloroplasts, or mitochondria. Two organelles were defined as being adjacent if they were separated by no more than 20 nm (the size of the gold particles used in these experiments). For these determinations of organelle proximity, 12 micrographs (one grid mesh square) of tissue labeled with anti-SGAT and 24 micrographs (two grid mesh squares) of tissue labeled with anti-ICL were examined. A nonparametric Mann-Whitney U test (23) was used to test for significant differences in labeling density between microbodies adjacent to other organelles.

RESULTS

Definition of the Transition Stage of Microbody Development

To study microbodies undergoing the transition from glyoxysomal to peroxisomal function, we first selected a stage of development characterized by high levels of both types of activities. The changes in activities of four microbody enzymes during the first 8 d of postgerminative development are shown in Fig. 1. The glyoxysomal marker enzymes ICL and MS rose from low levels of activity at day 1 to peak activities at day 3 or 4. Thereafter, both enzymes dropped in activity to low levels by day 8. This drop in activity occurred considerably faster in light-grown seedlings. The peroxisomal enzymes HPR and SGAT were detectable only at very low levels in dry seeds through day 2. Beginning at about day 3, these enzymes rose rapidly in the light to high levels by day 8. We have used quantitative immunossays for two of these enzymes, ICL and HPR, to show that changes in enzyme activity during this period are very accurate indicators of the changes in immunodetectable ICL and HPR protein (Wadle, D. M., and D. E. Titus, unpublished results).

These changes in enzyme activity were accompanied by specific ultrastructural changes in the cotyledonary spongy mesophyll and palisade cells. At day 2, lipid bodies and protein bodies occupied most of the cell volume, whereas proplastids and promitochondria were rare and indistinct (26). Microbodies were recognizable by their granular appearance (11). By day 8, the cell was vacuolate and the cytoplasm contained numerous chloroplasts and virtually no lipid bodies or protein bodies (26). The cells of day 4 cotyledonary tissue contained both lipid bodies and chloroplasts as well as high levels of glyoxysomal and peroxisomal enzymes. This tissue was therefore chosen as a suitable stage at which to study the transition in microbody function.

Antisera to ICL, MS, SGAT, and HPR Specifically Labeled Microbodies in Day 4 Tissue

The localization of ICL, MS, SGAT, and HPR in day 4, Lowicryl K4M-embedded cotyledonary tissue was performed by immunolabeling of thin sections. Sections were reacted with each specific antiserum (or the corresponding preimmune serum) followed by 20 nm protein A-gold. Fig. 2 illustrates that antisera to the glyoxysomal enzymes ICL (Fig. 2*a*) and MS (Fig. 2*c*) specifically labeled microbodies. Only low levels of gold particles were deposited over other cellular structures. Fig. 3 shows that the peroxisomal enzymes SGAT (Fig. 3*a*) and HPR (Fig. 3*c*) were similarly localized to microbodies in this tissue. The preimmune controls for all four antisera (Fig. 2, *b* and *d* and 3, *b* and *d*) exhibited no specific gold labeling.

A quantitative confirmation of the labeling specificity obtained with anti-ICL and anti-SGAT sera is provided in Table I. With our labeling conditions, microbodies contained a

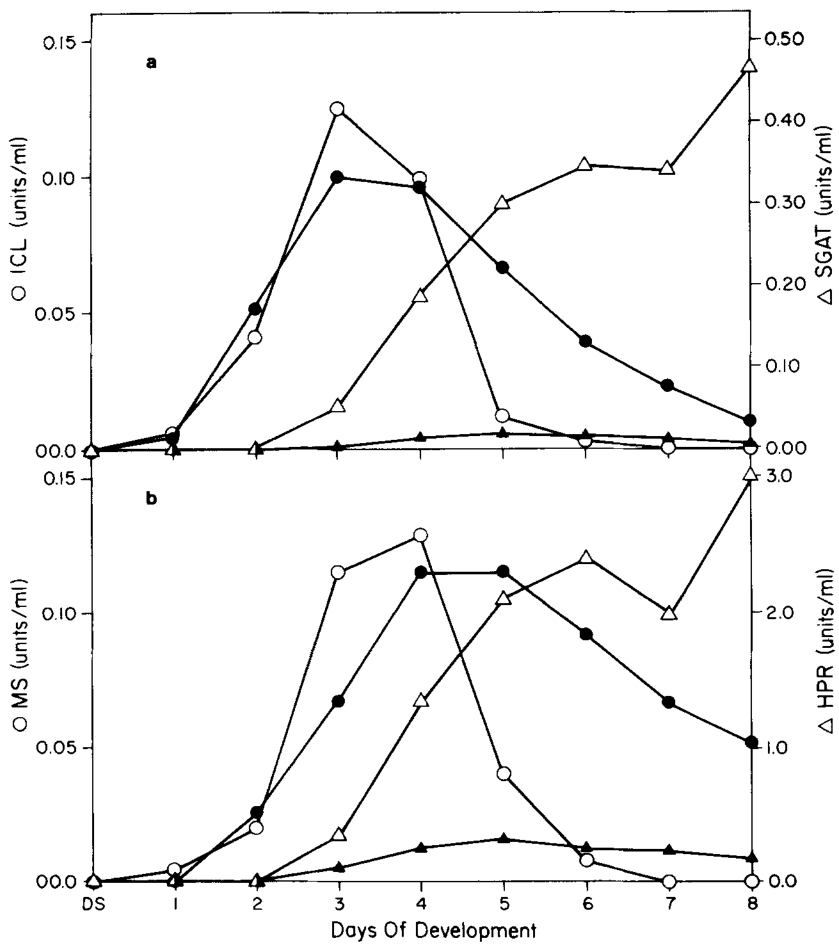

FIGURE 1 Activities of glyoxysomal and peroxisomal enzymes in cotyledons of light- and dark-grown seedlings. Activities of the glyoxysomal enzymes ICL (*a*, circles) and MS (*b*, circles) peak 3 to 4 d after germination and decline more rapidly in light-grown cotyledons (white circles) than in dark-grown cotyledons (black circles). Activities of the peroxisomal enzymes SGAT (*a*, triangles) and HPR (*b*, triangles) increase rapidly after day 2 in light-grown cotyledons (white triangles) but remain at low levels in dark-grown cotyledons (black triangles). *DS*, dry seeds.

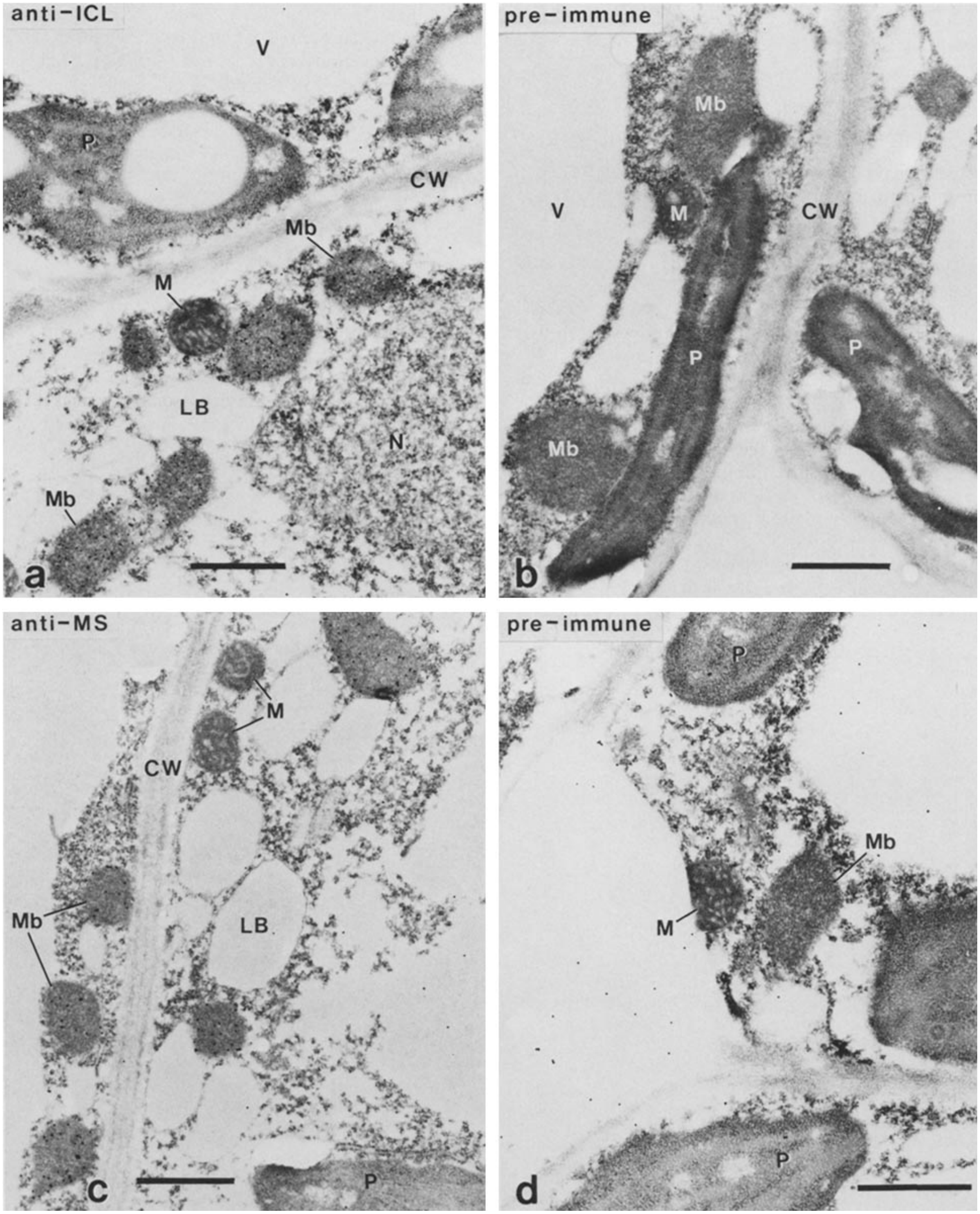

FIGURE 2 Localization of glyoxysomal enzymes in 4-d light-grown cotyledons. Sections of Lowicryl-embedded tissue slices were reacted with rabbit antiserum followed by 20 nm protein A-gold. (*a*) Labeling with anti-ICL serum; (*b*) labeling with the corresponding preimmune serum; (*c*) labeling with anti-MS serum; (*d*) labeling with the corresponding preimmune serum. *CW*, cell wall; *LB*, lipid body; *M*, mitochondrion; *Mb*, microbody; *N*, nucleus; *P*, chloroplast; *V*, vacuole. Bar, 1 μm. (*a–c*) $\times$ 16,000. (*d*) $\times$ 18,800.

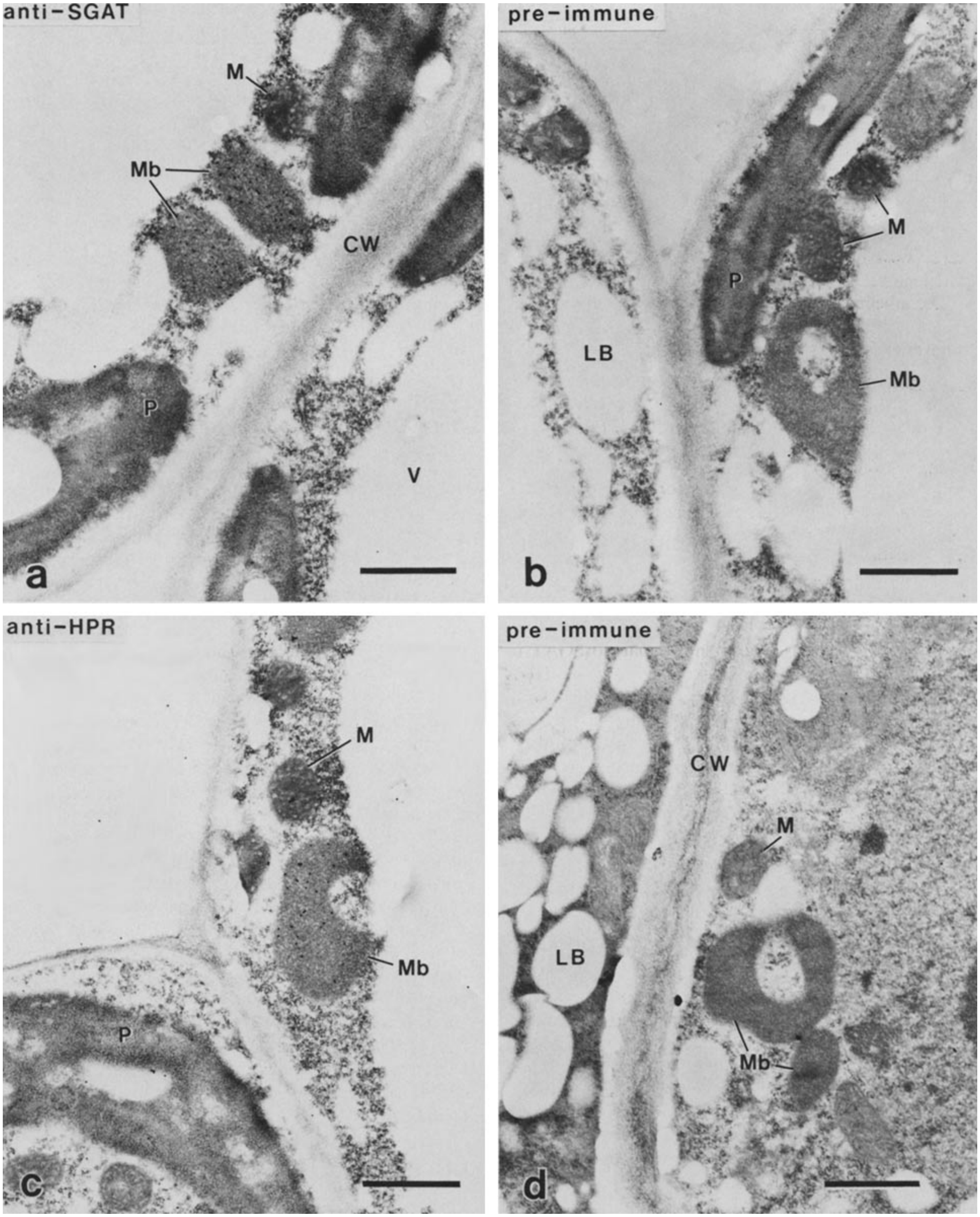

FIGURE 3 Localization of peroxisomal enzymes in 4-d light-grown cotyledons. Thin sections were reacted with rabbit antiserum followed by 20 nm protein A-gold. (*a*) Labeling with anti-SGAT serum; (*b*) labeling with the corresponding preimmune serum; (*c*) labeling with anti-HPR serum; (*d*) labeling with the corresponding preimmune serum. *CW*, cell wall; *LB*, lipid body; *M*, mitochondrion; *Mb*, microbody; *P*, chloroplast; *V*, vacuole. Bar, 1 μm. × 16,000.

TABLE I. *Specificity of Immunocytochemical Labeling*

Subcellular structure	Anti-ICL		Anti-SGAT	
	Average particles per μm^{2*}	Number of organelles examined	Average particles per μm^{2*}	Number of organelles examined
Microbodies	66.4 ± 25.4	91	54.6 ± 25.0	43
Lipid bodies	0.03 ± 0.17	86	0.79 ± 3.20	83
Chloroplasts	0.29 ± 0.33	22	1.62 ± 1.00	32
Mitochondria	0.46 ± 1.72	33	4.24 ± 9.51	33
Cytoplasm + cell wall	0.17 ± 0.09	—	0.36 ± 0.00	—
Vacuole	0.07 ± 0.05	—	0.34 ± 0.35	—

* Particle densities are expressed as mean ± SD.

mean density of 66.4 ± 25.4 and 54.6 ± 25.0 gold particles/μm^2 when labeled with anti-ICL and anti-SGAT sera, respectively. The labeling densities over lipid bodies, chloroplasts, mitochondria, vacuoles, cytoplasm, and cell walls were much lower, never exceeding 4.2 particles/μm^2.

Developmental Stages Which Lacked Enzyme Activity Also Lacked Immunocytochemical Staining for That Enzyme

Further confirmation that the immunolabeling observed at day 4 genuinely reflected the presence of these enzymes was obtained by examining developmental stages in which a given enzyme was known to be either absent or present at very low levels. Immunolabeling was performed with all four sera at day 2, when SGAT and HPR were nearly undetectable by enzymatic assays, and at day 8, when ICL and MS activities had dropped to low levels. Fig. 4 shows that no SGAT or HPR could be detected immunocytochemically in day 2 tissue, whereas antisera to ICL and MS readily labeled microbodies. Fig. 5 illustrates the analogous control experiment with tissue from eight day cotyledons. As expected, antisera to ICL and MS showed no appreciable gold labeling, whereas antisera to SGAT and HPR strongly labeled microbodies. Preimmune controls (not shown) revealed no specific gold labeling in either day 2 or day 8 tissue.

Double-label Immunocytochemistry with Anti-ICL and Anti-SGAT Sera

Optimum results could be obtained at higher dilutions of anti-ICL and anti-SGAT sera (1:2,000 and 1:200, respectively) than with antisera to MS and HPR (1:100 dilution). Accordingly, anti-ICL and anti-SGAT sera were used for double-label immunocytochemistry to minimize the nonspecific gold deposition to which these experiments are prone. Thin sections from day 4 cotyledons were incubated with anti-ICL serum and 10 nm protein A-gold followed by anti-SGAT serum and 20 nm protein A-gold. Fig. 6*a* shows that microbodies were labeled with substantial amounts of both small and large gold particles.

When preimmune serum was substituted for anti-SGAT serum, labeling with large (20 nm) gold was sharply reduced over microbodies (Fig. 6*b*). Similarly, the substitution of preimmune serum for anti-ICL serum resulted in no deposition of small (10 nm) gold over microbodies (Fig. 6*c*). Fig. 7 illustrates the results when the order of labeling was reversed such that incubation with anti-SGAT serum and 10 nm protein A-gold preceded incubation with anti-ICL serum and 20 nm protein A-gold. Once again, microbodies exhibited labeling with both sizes of gold (Fig. 7*a*) and substitution of preimmune sera for either anti-ICL serum (Fig. 7*b*) or anti-SGAT serum (Fig. 7*c*) resulted in greatly reduced deposition of the corresponding size of gold.

Quantitation of Protein A-Gold Deposition in Microbodies Adjacent to Lipid Bodies, Chloroplasts, and Mitochondria

Labeling with both sizes of gold was observed in virtually all microbodies examined in day 4 tissue. No significant differences in labeling intensity were apparent in microbodies adjacent to lipid bodies as compared to chloroplasts. The latter point was not quantitated in the double-labeled tissue because the high magnification needed to see the smaller size gold particles necessarily restricted the number of microbodies that could be examined. Instead, quantitation of gold labeling was performed at lower magnification on sections that had been labeled with either anti-ICL or anti-SGAT serum followed by 20 nm protein A-gold. The density of gold particles was measured over microbodies that were adjacent to lipid bodies, chloroplasts, mitochondria, or combinations of these organelles, as well as over microbodies adjacent to none of these organelles (Table II).

Microbodies that were labeled with anti-ICL antiserum and that were adjacent to lipid bodies, to chloroplasts, or to both organelles exhibited gold particle densities of 65.9 ± 27.3, 54.6 ± 16.9, and 79.0 ± 22.9, respectively. Gold particle densities over microbodies labeled with anti-SGAT antiserum were 62.0 ± 29.1, 52.1 ± 31.7, and 55.3 ± 22.7 in these respective categories. All pairwise comparisons within each group of three categories were made. Five out of the six comparisons indicated no significant difference in labeling density. The difference in labeling density between anti-ICL-labeled microbodies adjacent to chloroplasts and those adjacent to both lipid bodies and chloroplasts was significant at the 0.05 level.

DISCUSSION

Three models have been proposed to explain the transition from glyoxysomal to peroxisomal function in microbodies of developing cotyledons of cucumbers and other oilseeds. Beevers (2) and Kagawa and Beevers (14) have postulated that this transition is accomplished by the destruction of glyoxysomes and simultaneous synthesis of microbodies containing peroxisomal activities. This model, known as the two-population (or replacement) model, predicts that glyoxysomal and per-

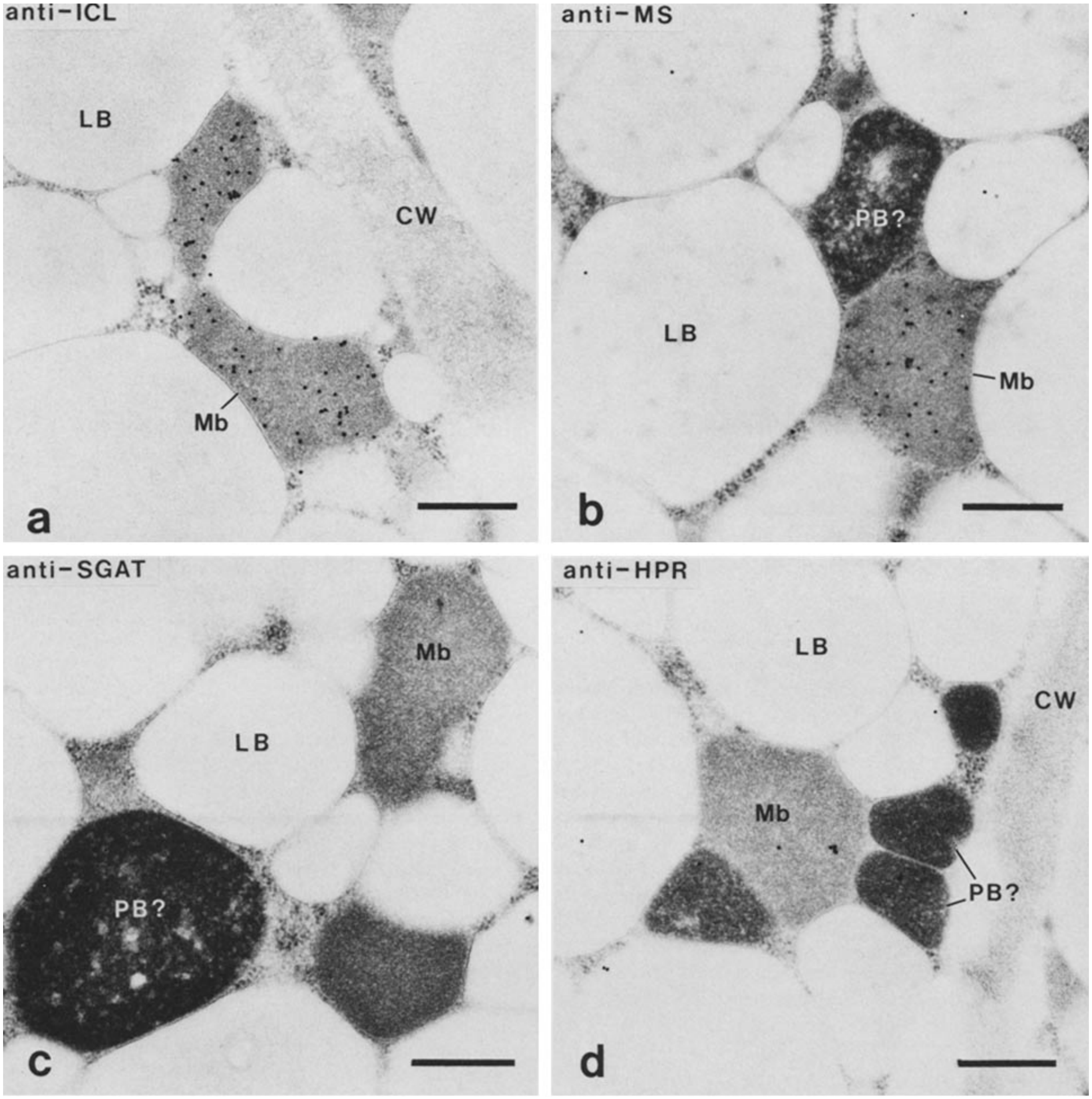

FIGURE 4 Immunocytochemical detection of glyoxysomal enzymes, but not peroxisomal enzymes, in 2-d light-grown cotyledons. Labeling was performed with antisera directed against the glyoxysomal enzymes ICL (*a*) and MS (*b*), or the peroxisomal enzymes SGAT (*c*) and HPR (*d*). Control labelings with preimmune sera (not shown) yielded only low, nonspecific deposition of gold particles. *CW*, cell wall; *LB*, lipid body; *Mb*, microbody; *PB?*, possible protein body. Bar, 0.5 μm. × 30,000.

oxisomal marker enzymes will be found in separate organelle populations during the transition period and that glyoxysomal lipids and proteins will undergo substantial turnover. Such turnover should include catalase and other enzymes common to glyoxysomes and peroxisomes.

Burke and Trelease (6) and Trelease et al. (26) have suggested that this transition in microbody function occurs by the gradual replacement of glyoxysomal enzymes with peroxisomal enzymes in a continually intact microbody membrane. This model, termed the one-population (or repackaging) model, predicts that glyoxysomal and peroxisomal marker enzymes will co-exist within individual microbodies during the transition period and that a substantial turnover of microbody membranes and of proteins such as catalase need not occur. More recently, Schopfer et al. (21) have proposed an alternative which is called the glyoxyperoxisome (or enzyme synthesis changeover) model (22). This model suggests that glyoxysomal and peroxisomal enzymes co-exist in microbodies during the transition stage but differs from the one-population model in that the change in enzyme composition would be accomplished by a continual turnover of microbodies, with the enzyme content of each microbody determined by the specific complement of microbody proteins being synthesized when that microbody is formed.

The three models have provided a useful framework for examining the transition in microbody function. The one-population model could be disproven by the clear demonstration of turnover of entire glyoxysomes. Kagawa et al. (15, 16) have provided evidence for turnover of microbody membrane lipids at the transition stage, but Trelease et al. (26) could find

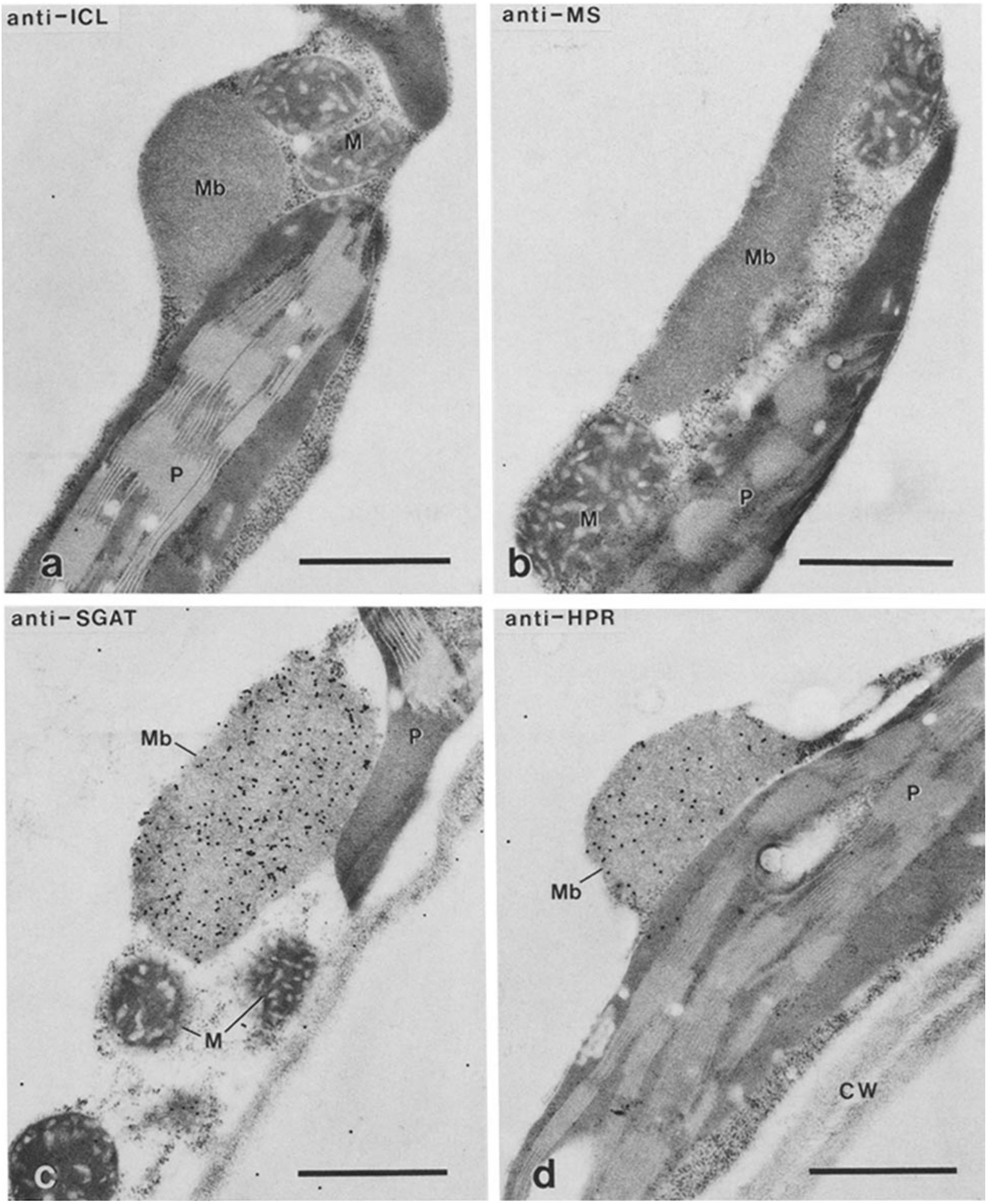

FIGURE 5 Immunocytochemical detection of peroxisomal enzymes, but not glyoxysomal enzymes, in 8-d light-grown cotyledons. Labeling was performed with antisera directed against the glyoxysomal enzymes ICL (*a*) and MS (*b*), or the peroxisomal enzymes SGAT (*c*) and HPR (*d*). Control labelings with preimmune sera (not shown) yielded only low, nonspecific deposition of gold particles. *CW*, cell wall; *M*, mitochondrion; *Mb*, microbody; *P*, chloroplast. Bar, 1 μm. × 25,000.

no ultrastructural evidence for microbody turnover. Neither finding constitutes definitive evidence for a given model. Betsche and Gerhardt (3) have shown that the rate of catalase synthesis at the transition stage is too low to account for a complete turnover of glyoxysomal catalase, supporting the notion that glyoxysomes are repackaged with peroxisomal enzymes and that some of the glyoxysomal catalase is reused in this process.

The two-population model depends on the assertion that glyoxysomal and peroxisomal enzymes reside in separate populations. Attempts to resolve such populations by subcellular fractionation have not yielded definitive results (5, 9).

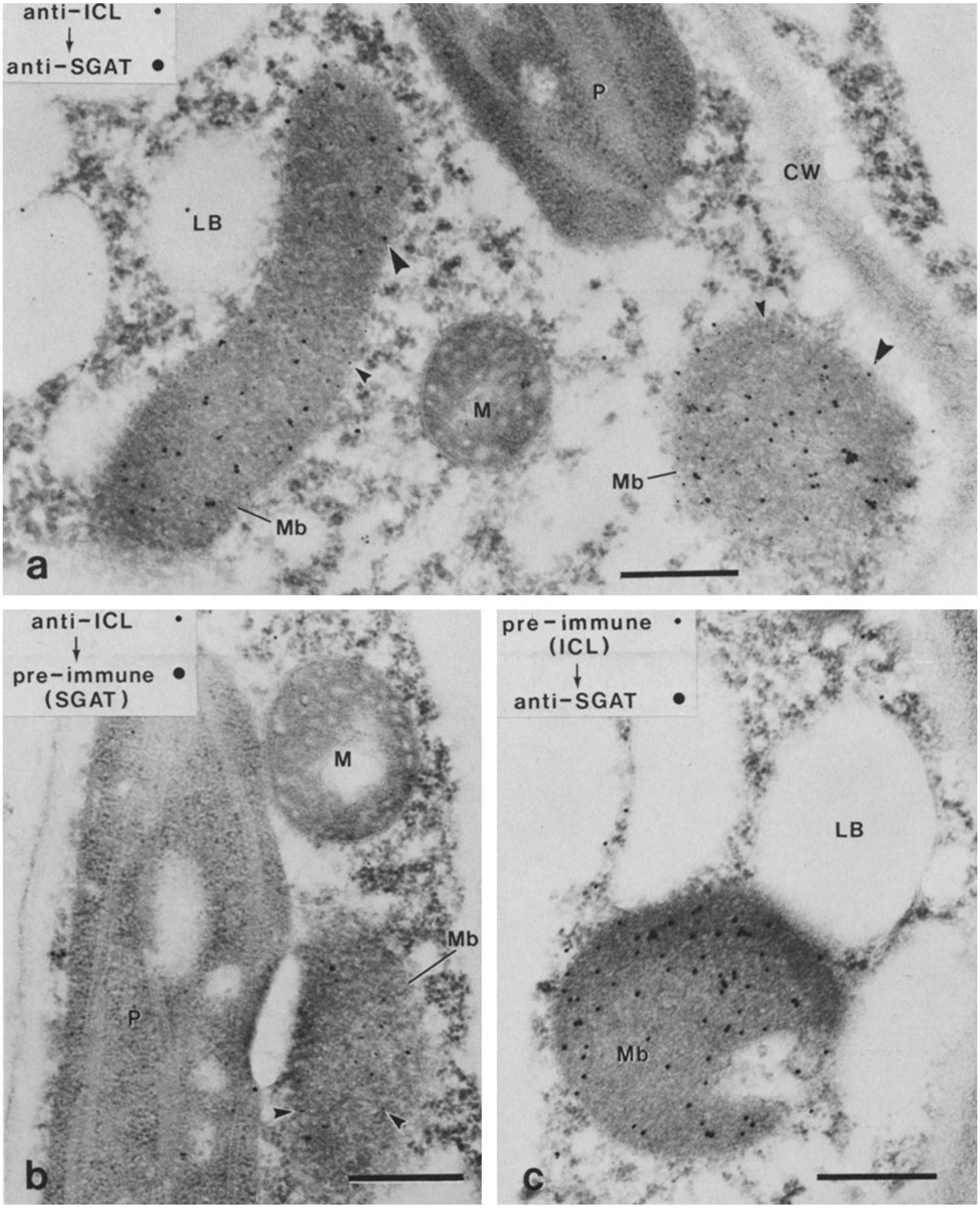

FIGURE 6 Double-label immunocytochemical detection of ICL and SGAT in 4-d light-grown cotyledons. (*a*) Labeling with anti-ICL serum and 10 nm protein A-gold (small arrowheads) followed by anti-SGAT serum and 20 nm protein A-gold (large arrowheads); (*b*) substitution of preimmune serum for anti-SGAT; (*c*) substitution of preimmune serum for anti-ICL. *CW*, cell wall; *LB*, lipid body; *M*, mitochondrion; *Mb*, microbody; *P*, chloroplast. Bar, 0.5 μm. × 40,000.

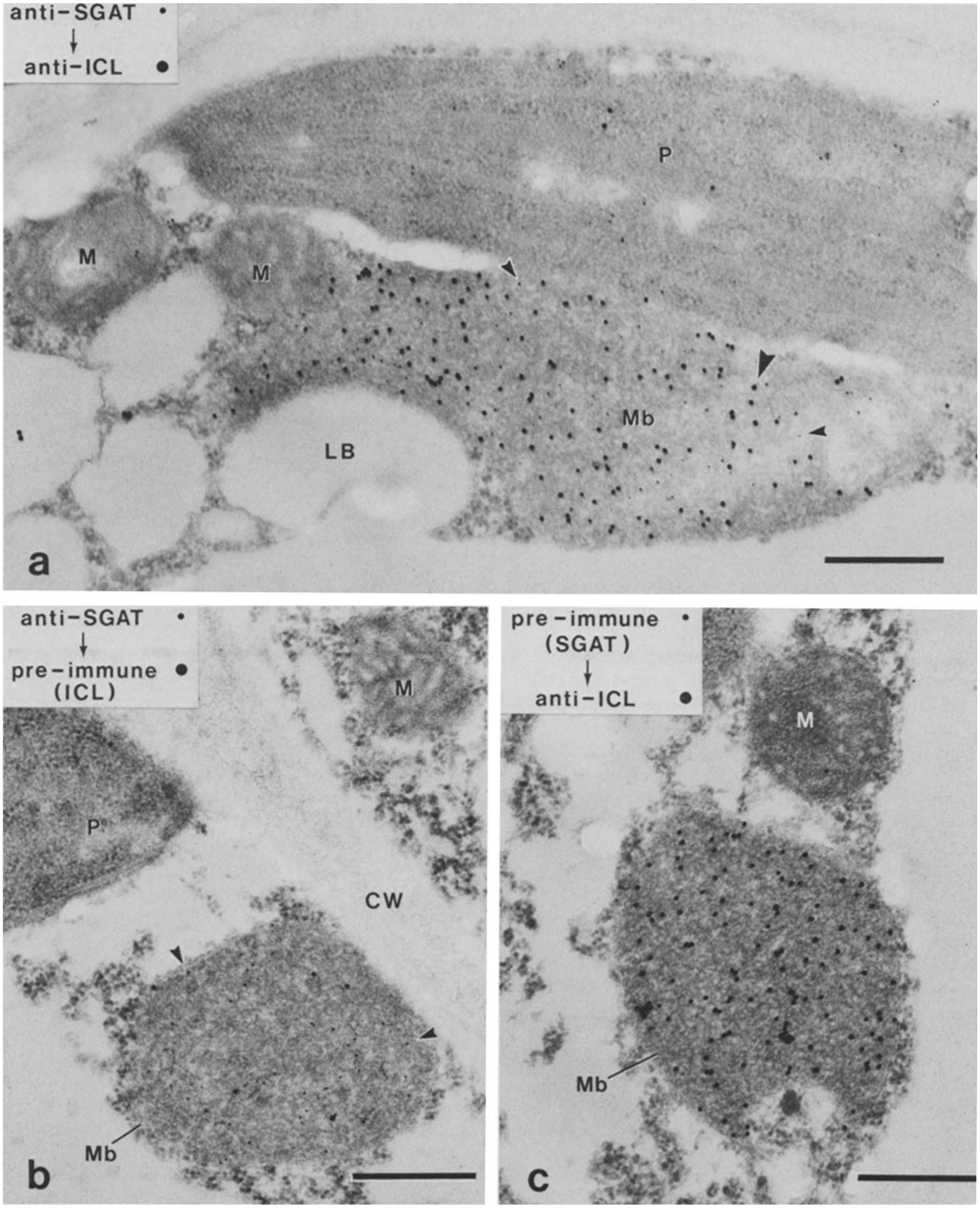

FIGURE 7 Double-label immunocytochemical detection of SGAT and ICL in 4-d light-grown cotyledons. (a) Labeling with anti-SGAT serum and 10 nm protein A-gold (small arrowheads) followed by anti-ICL serum and 20 nm protein A-gold (large arrowheads); (b) substitution of preimmune serum for anti-ICL; (c) substitution of preimmune serum for anti-SGAT. *CW*, cell wall; *LB*, lipid body; *M*, mitochondrion; *Mb*, microbody; *P*, chloroplast. Bar, 0.5 μm. $\times$ 40,000.

TABLE II. *Immunocytochemical Labeling of Microbodies Adjacent to Lipid Bodies, Chloroplasts, and Mitochondria*

Microbodies adjacent to	Anti-ICL: Average particles per μm^{2*}	Anti-ICL: Number of organelles examined	Anti-SGAT: Average particles per μm^{2*}	Anti-SGAT: Number of organelles examined
Lipid bodies only	$65.9 \pm 27.3^{\ddagger\S}$	42	$62.0 \pm 29.1^{\P**}$	11
Chloroplasts only	$54.6 \pm 16.9^{\ddagger\|}$	10	$52.1 \pm 31.7^{\P\ddagger\ddagger}$	9
Mitochondria only	62.6 ± 44.4	2	36.0 ± 0.0	1
Lipid bodies + chloroplasts	$79.0 \pm 22.9^{\S\|}$	11	$55.3 \pm 22.7^{**\ddagger\ddagger}$	10
Lipid bodies + mitochondria	76.4 ± 15.5	6	61.7 ± 0.0	1
Chloroplasts + mitochondria	90.9 ± 0.0	1	45.2 ± 0.8	2
None of these	62.4 ± 25.8	19	50.5 ± 21.3	9

* Particle densities are expressed as mean ± SD. Pairs of density values with the same superscript were subjected to a nonparametric Mann-Whitney U test. *P* values corresponding to each comparison were as follows: $\ddagger$, 0.27; $\S$, 0.16; $\|$, 0.045; $\P$, 0.40; $**$, 0.86; $\ddagger\ddagger$, 0.65.

In contrast, Burke and Trelease (6) provided positive evidence for a single population by using cytochemical staining for MS and GO. In microbodies isolated from transition-stage cotyledonary tissue, 94 and 97% of microbodies were stained for MS and GO, respectively, suggesting that these enzymes coexist in individual microbodies and that the two-population model is therefore invalid.

Although these cytochemical results seem straightforward, several weaknesses have been pointed out, and the findings have not been regarded as conclusive. A definitive demonstration of MS and GO in the same microbody was not possible because the two cytochemical staining reactions were necessarily performed in different tissue blocks. Beevers (2) noted that significant background deposition of reaction product was evident on nonmicrobody membrane vesicles as well as in control stainings. This makes the identification of positively stained microbodies in the impure microbody fraction difficult and casts some doubt on the accuracy of the resultant quantitation. Schopfer et al. (21) and Schopfer and Apel (22) have claimed that GO is a poor choice for a peroxisomal marker enzyme because it is also present at low levels in glyoxysomes. Since other peroxisomal enzymes (e.g., SGAT, HPR) are also found in small amounts at early stages of development, a better criterion for a peroxisomal enzyme would be the characteristic light-dependent rise in activity after day 3.

To confirm that the transition-stage GO staining observed by Burke and Trelease (6) represents peroxisomal function, comparatively low levels of GO staining would need to be demonstrated in microbodies at day 1 or 2 when GO activity is presumably confined to glyoxysomes. Such quantitation of staining intensity over individual microbodies is probably not possible with enzyme cytochemistry, but can be performed with protein A-gold immunocytochemistry (7, 10, 18). Our data show that immunocytochemical labeling intensity is at least capable of reflecting large changes in enzyme activities (Figs. 4 and 5). In addition, our observation that virtually all microbodies in day 4 tissue are labeled with each of the four antisera clearly confirms the analogous observations of Burke and Trelease (6) concerning their transition-stage tissue.

Using double-label immunocytochemistry, we have been able to demonstrate directly the co-existence of a glyoxysomal and a peroxisomal enzyme within individual microbodies of transition-stage cucumber cotyledons. This evidence contradicts a central assertion of the two-population (replacement) model (2) and therefore provides strong support for the alternative models of the glyoxysome-peroxisome transition (21, 26).

The specificity of labeling was verified by two important control observations which demonstrated loss of labeling in the absence of specific antibody (preimmune controls) and in the absence of antigen (day 2 and 8 controls). Figs. 6*b* and 7*b* show that deposition of 20 nm gold particles is sharply reduced (though not entirely eliminated) when a preimmune serum is substituted for the second stage of a double-labeling experiment. This low level of labeling appeared to be specific for microbodies and did not occur when the preimmune serum was used first. A possible explanation for this phenomenon is that a few immunoglobulin molecules bound to microbodies in the first antiserum incubation may have been incompletely masked during the subsequent incubations with 10 nm protein A-gold and soluble protein A, and might thus have been available for binding by 20 nm protein A-gold.

We have also used immunocytochemistry to address experimentally the assumption of Schopfer et al. (21, 22) that a microbody can be identified as a glyoxysome or a peroxisome solely on the basis of its association with a lipid body or a chloroplast, respectively. According to these criteria, the proportion of microbodies in contact with both a lipid body and a chloroplast can be used to predict the proportion of microbodies which contain both glyoxysomal and peroxisomal activities and are undergoing the functional transition. Our evidence fails to confirm this assumption, but cannot rule out such a possibility.

Microbodies adjacent to both a lipid body and a chloroplast do indeed contain both ICL and SGAT, but the same is true of microbodies adjacent only to a lipid body, a chloroplast, a mitochondrion, or none of these organelles. If Schopfer's assumption (21) were true, ICL might be expected to be concentrated in microbodies adjacent to lipid bodies, SGAT might be concentrated in microbodies adjacent to chloroplasts, and both enzymes would be expected to be present at relatively high levels in microbodies adjacent to both lipid bodies and chloroplasts. However, with one exception, quantitation of immunocytochemical labeling for ICL or SGAT in day 4 tissue revealed no significant differences in protein A-gold density over microbodies in these categories. One interpretation of this homogeneity of labeling density might be that every microbody in a day 4 cotyledon is adjacent to both a lipid body and a chloroplast at some point in the cell. While this interpretation is consistent with Schopfer's proposal, we feel that the possible functional significance of microbody associations with other organelles is still an open question since the correlation of microbody enzyme activities and organelle associations has been described only at a populational level and not for individual microbodies.

We wish to express our gratitude to Dr. Eldon Newcomb and the members of his laboratory for the use of their electron miocroscope facility and for much helpful advice. We thank Dr. Jürgen Roth (Biozentrum, University of Basel, Basel, Switzerland), Dr. Barbara Armbruster (Washington University Medical School, St. Louis, MO), and Dr. Craig R. Lending (University of California, Riverside, CA) for helpful advice on immunocytochemical procedures; David Hondred and Dawn-Marie Wadle for help with experiments described in Fig. 1; Jeff Hoyer, Karen Agee, Kevin Murphy, and Doug Levey for technical assistance with quantitation of immunocytochemical labeling; and Lucy Taylor and Claudia Lipke for help with preparation of figures.

This work was supported by National Science Foundation grant PCM83-08195.

Received for publication 25 February 1985, and in revised form 7 May 1985.

Note Added in Proof: Since submission of this manuscript, we have become aware of a report by C. Sautter (*J. Ultrastruct. Res.*, 1984, 89:187–197) in which the protein A–gold technique was used for the immunocytochemical localization of ICL and HPR to microbodies in watermelon cotyledons, but without addressing the question of the glyoxysome-peroxisome transition.

REFERENCES

1. Becker, W. M., C. J. Leaver, E. M. Weir, and H. Riezman. 1978. Regulation of glyoxysomal enzymes during germination of cucumber. I. Developmental changes in cotyledonary protein, RNA, and enzyme activities during germination. *Plant Physiol. (Bethesda).* 62:542–549.
2. Beevers, H. 1979. Microbodies in higher plants. *Ann. Rev. Plant Physiol.* 30:159–193.
3. Betsche, T., and B. Gerhardt. 1978. Apparent catalase synthesis in sunflower cotyledons during the change in microbody function. A mathematical approach for the quantitative evaluation of density-labeling data. *Plant Physiol. (Bethesda).* 62:590–597.
4. Breidenbach, R. W., and H. Beevers. 1967. Association of the glyoxylate cycle enzymes in a novel subcellular particle from castor bean endosperm. *Biochem. Biophys. Res. Commun.* 27:462–469.
5. Brown, R. H., and M. J. Merrett. 1977. Density labelling during microbody development in cotyledons. *New Phytol.* 79:73–81.
6. Burke, J. J., and R. N. Trelease. 1975. Cytochemical demonstration of malate synthetase and glycolate oxidase in microbodies of cucumber cotyledons. *Plant Physiol. (Bethesda).* 56:710–717.
7. Doman, D. C., and R. N. Trelease. 1985. Protein A-gold immunocytochemistry of isocitrate lyase in cotton seeds. *Protoplasma.* 124:157–167.
8. Frens, G. 1973. Controlled nucleation for the regulation of the particle size in monodisperse gold suspensions. *Nature Phys. Sci.* 241: 20–22.
9. Gerhardt, B. 1973. Untersuchungen zur Funktionsänderung der Microbodies in den Keimblättern von *Helianthus annuus* L. *Planta (Berl.).* 110:15–28.
10. Geuze, H. J., J. W. Slot, G. J. A. M. Strous, H. F. Lodish, and A. L. Schwartz. 1983. Intracellular site of asialoglycoprotein receptor-ligand uncoupling: double-label immunoelectron microscopy during receptor-mediated endocytosis. *Cell.* 32:277–287.
11. Gruber, P. J., R. N. Trelease, W. M. Becker, and E. H. Newcomb. 1970. A correlative ultrastructural and enzymatic study of cotyledonary microbodies following germination of fat-storing seeds. *Planta (Berl.).* 93:262–288.
12. Hondred, D., J. McC. Hunter, R. Keith, D. E. Titus, and W. M. Becker. 1985. Isolation of serine:glyoxylate aminotransferase from cucumber cotyledons. *Plant Physiol. (Bethesda).* In press.
13. Horisberger, M. 1979. Evaluation of colloidal gold as a cytochemical marker for transmission and scanning electron microscopy. *Biol. Cell.* 36:253–258.
14. Kagawa, T., and H. Beevers. 1975. The development of microbodies (glyoxysomes and peroxisomes) in cotyledons of germinating watermelon seedlings. *Plant Physiol. (Bethesda).* 55:258–264.
15. Kagawa, T., J. M. Lord, and H. Beevers. 1973. The origin and turnover of organelle membranes in castor bean. *Plant Physiol. (Bethesda).* 51:61–65.
16. Kagawa, T., J. M. Lord, and H. Beevers. 1975. Lecithin synthesis during microbody biogenesis in watermelon cotyledons. *Arch. Biochem. Biophys.* 167:45–53.
17. Lamb, J. E., H. Riezman, W. M. Becker, and C. J. Leaver. 1978. Regulation of glyoxysomal enzymes during germination. II. Isolation and immunological detection of isocitrate lyase and catalase. *Plant Physiol. (Bethesda).* 62:754–760.
18. Posthuma, G., J. W. Slot, and H. J. Geuze. 1984. Immunocytochemical assays of amylase and chymotrypsinogen in rat pancreas secretory granules. Efficacy of using immunogold-labeled ultrathin cryosections to estimate relative protein concentrations. *J. Histochem. Cytochem.* 32:1028–1034.
19. Riezman, H., E. M. Weir, C. J. Leaver, D. E. Titus, and W. M. Becker. 1980. Regulation of glyoxysomal enzymes during germination of cucumber. III. In vitro translation and characterization of four glyoxysomal enzymes. *Plant Physiol. (Bethesda).* 65:40–46.
20. Roth, J., and M. Binder. 1978. Colloidal gold, ferritin and peroxidase as markers for electron microscopic double labeling lectin techniques. *J. Histochem. Cytochem.* 26:163–169.
21. Schopfer, P., D. Bajracharya, R. Bergfeld, and H. Falk. 1976. Phytochrome-mediated transformation of glyoxysomes into peroxisomes in the cotyledons of mustard seedlings. *Planta.* 133:73–80.
22. Schopfer, P., and K. Apel. 1983. Intracellular photomorphogenesis. *In* Encyclopedia of Plant Physiology, New Series. W. Schropshire, Jr. and H. Mohr, editors. Springer-Verlag, Berlin/Heidelberg. 258–288.
23. Siegel, S. 1956. Nonparametric statistics for the behavioral sciences. McGraw-Hill, New York.
24. Titus, D. E., D. Hondred, and W. M. Becker. 1983. Purification and characterization of hydroxypyruvate reductase from cucumber cotyledons. *Plant Physiol. (Bethesda).* 72:402–408.
25. Tolbert, N. E., A. Oeser, T. Kisaki, R. H. Hageman, and R. K. Yamazaki. 1968. Peroxisomes from spinach leaves containing enzymes related to glycolate metabolism. *J. Biol. Chem.* 243:5179–5184.
26. Trelease, R. N., W. M. Becker, P. J. Gruber, and E. H. Newcomb. 1971. Microbodies (glyoxysomes and peroxisomes) in cucumber cotyledons. A correlative biochemical and ultrastructural study in light and dark grown seedlings. *Plant Physiol. (Bethesda).* 48:461–475.